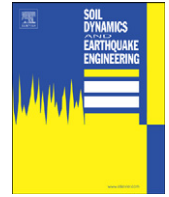




Contents lists available at ScienceDirect

Soil Dynamics and Earthquake Engineering

journal homepage: www.elsevier.com/locate/soildyn



Should average shear-wave velocity in the top 30 m of soil be used to describe seismic amplification?

Vincent W. Lee, Mihailo D. Trifunac*

Civil Engineering Department, University of Southern California, Los Angeles, CA 90089-2531, USA

ARTICLE INFO

Article history:

Received 11 April 2009
Received in revised form
9 May 2010
Accepted 10 May 2010

ABSTRACT

The average velocity of shear waves in the top 30 m of soil, v_L , has become the parameter used by many engineering design codes and most recently by published empirical-scaling equations to estimate the amplitudes of strong ground motion. Yet there are few studies to determine whether this is a meaningful parameter to use—and whether estimates that do use it are reliable. In 1995, the authors studied this problem and concluded that v_L should not be used. We reported then that an older site characterization in terms of the soil site parameter proposed by Seed et al. [1], s_L , worked better because it included a measure of the thickness of the soil layers to considerably greater depths. Our report, however, made no difference; numerous papers continued to be published based only on scaling in terms of v_L , and worse, they also ignored the geological site conditions. The purpose of this paper is to emphasize that the average shear-wave velocity in the top 30 m of soil should not be the only site parameter used to scale strong-motion amplitudes. While the search continues for the more meaningful site parameters to use in empirical scaling of strong earthquake ground motion, it is better to use s_L to describe the amplification of seismic waves by soil deposits near the surface.

© 2010 Elsevier Ltd. All rights reserved.

1. Introduction

Examples of the early investigations of the effects of site conditions on the amplitudes of strong earthquake ground motion can be found in the papers of Reid [2] and Sezawa et al. [3]. These studies emerged from the attempts to explain observations of damage caused by earthquakes. Theoretical studies of linear-wave propagation, showing amplification as seismic waves propagating from “hard” into “soft” deposits, contributed to a view that the strong-motion shaking should be amplified in the soft surface soils. This view prevailed for many years and is evident in the formulation of early design codes [4], and in the guidelines for the design of important structures [5]. Kanai's descriptions of the patterns of damage to Japanese wooden houses, for example, reveal his appreciation for many conflicting observations [6], but in the end the simplifications needed for the development of design codes prevailed. The absence of recorded strong-motion accelerograms by dense arrays prior to the 1970s [7,8], and the lack of three-dimensional soil and geological characterizations of sites, eventually led to simplified site descriptions, many of which continue to be used today.

Looking back at the studies of site effects, certain trends emerge. First, many studies were carried out by prominent

seismologists (e.g., [9]), who at first could work only with linear waves, with long-period motions (say, longer than ~ 1 s), small wave amplitudes, and large epicentral distances (e.g., more than ~ 100 km). Second, engineering contributions to the studies of site effects, in the beginning, used only the amplitudes of peak acceleration (i.e., they did not consider the frequency content of ground motion) and tended to use only the site characterization in terms of the surface soil conditions (with dimensions rarely exceeding ~ 200 m (e.g., [1,10,11])). Third, with few exceptions, most studies employed forward modelling and regression analyses and rarely tested the significance of the computed regression coefficients or the significance of the cross-correlations among the parameters of the model. For example, the soil site-condition variables (which are expected to be more important for short-period motions) and the geologic site-condition variables (expected to be important for intermediate and long-period motion) are correlated by the nature of their formation, but are usually not considered simultaneously in most regression models. The result is that most scaling methods, which are based on the site conditions and consider only soil-site classification, average out the effects of the geological site conditions and are characterized by large uncertainty in the prediction of spectral amplitudes. Fourth, because most strong-motion data are available for fault-to-station distances in the range from 25 to 100 km, all published regression models essentially reflect the trends in the data for this distance range. Since the significant damage to structures occurs mainly within several tens of kilometres from

* Corresponding author.

E-mail address: trifunac@usc.edu (M.D. Trifunac).

the fault (in the near field), the nature of the site effects and the extent to which they influence the ground motion will be different from what is determined from the regression analyses of the distant recordings, which describe essentially linear and almost-linear site response. Fifth, it is assumed that the site effects are repeatable from one earthquake to the next and do not depend significantly upon the azimuth, angle of incidence, and amplitudes of seismic waves. However, studies of multiple earthquake recordings at the same strong-motion stations show that this assumption holds at best only about 50% of the time, only at some recording stations [12–14], and depends on the peak strains accompanying the strong motion [15]. Sixth, it is rarely asked whether the parameterisation of the site conditions should have been done differently, on the basis of some rational physical considerations, so that it correlates with and is significant in terms of the end result like distribution of damage, for example. Clearly, the damage of structures also depends on other characteristics of strong motion, like duration [16], Q factor in the layers near ground surface [17], and the rate of energy input into the structure [18], but the data on damage includes consequences of all relevant physical factors, which lead to the observed state, and is therefore most relevant for engineering process parameterisation [19–24]. Seventh, site effects (amplification) are not only related to free field site conditions, but can be caused by two- and three-dimensional wave propagation phenomena like scattering, interference, and diffraction [25–31], and in urban areas by scattering from large foundations and underground structures [32–34]. The motions recorded at “free field sites”, in the vicinity of large building foundations can be affected by the nonlinear soil structure interaction and by the relative rigidity of the foundations [35–38]. Eighth, the seismic energy is not radiated only from the fault, but also from the volume surrounding the fault, and therefore the peak amplitudes of strong motion occur at some distance from the fault [39]. This makes the regression studies of the site effects in terms of simple attenuation models complicated, because the nature of the attenuation is different in the near and in the far field. At short distances from the fault, peak acceleration practically does not depend on distance or on magnitude [40–43], and the effects of site conditions, which can be seen at distances greater than the source dimension, are not present because of the large strains in the near field [44] and nonlinear site response [45–50].

Licensing pressures ensuing from the need for consensus building among ground-motion experts—first in the design of nuclear power plants and then in the revision of the design codes—have resulted in the emergence of group efforts for the development of scaling equations of strong ground motion. On the positive side, this has culminated in an increased exchange of ideas and more discussions among researchers who work on the effects of local site conditions. However, this has also reduced the role of individual approaches and has led to the adoption of scaling models that favour the “average” view rather than the search for the “best” physical models. This consensus building may help to speed up the licensing process, but nature will follow its course: what individual researchers may not be able to change in the consensus, future earthquakes certainly will. In the following, we will not be guided by any “consensus” views but rather will try to examine what can be learned from the data, and how local site effects should be described to improve their significance in the empirical scaling equations.

Physically realistic descriptions of the local site conditions are directly or indirectly essential for meaningful formulation of models and modelling parameters in many engineering analyses of ground and structural response. Through the Fourier spectrum amplitudes (e.g., [51]), site conditions play a decisive role in influencing the outcome in the synthesis of artificial strong-

motion accelerograms (e.g., [52,53]), in the nature of structural response [54–56] and in determining the threshold for the occurrence of liquefaction [57], for example. By influencing the wavelengths of excitation, the site conditions determine the relative significance of differential ground motions on the response of extended structures [58–61]. For large strong-motion amplitudes, the nature of nonlinear response—near ground surface, in shallow sediments and in soils—can play a decisive role in governing the extent and the geographical distribution of earthquake damage [62–64].

2. The linear approach

Transfer-function representation of strong motion can be viewed in the frequency domain as

$$O(f) = E(f)P(f)S(f) \quad (1)$$

where f is the frequency, $O(f)$ and $E(f)$ are the Fourier spectra of the motion at a site and at the earthquake source, and $P(f)$ and $S(f)$ are the transfer functions of the propagation path and of the local site effects. This representation is meaningful for epicentral distances that are large relative to the source dimensions, when the earthquake source can be approximated by a point source. In the near field, the small distance results in geometrical nonlinearities caused by the spatial distribution of wave arrivals from different segments of the fault surface. In the near field, Eq. (1) ceases to be valid because $E(f)$, $P(f)$, and $S(f)$ become complex, geometrically nonlinear functions of the space coordinates. While $O(f)$ could be represented by an equation related to Eq. (1), it would have to be in the form of an integral over the fault surface, with $P(f)$ and $S(f)$ being functions that depend upon the geologic environment and upon the site location. Further, $E(f)$ would have to include contributions from near-field terms in the source radiation ($1/r^2$ and $1/r^4$ terms, where r is the distance between the site and a point on the fault surface; [65,66]). With $R/a \rightarrow \infty$, where R is the epicentral distance and a is some representative size of asperities on the fault surface, Eq. (1) asymptotically becomes linear (geometrically, because there is no need to integrate over the fault surface) and can represent the site and the propagation effects well.

For two sites having different site conditions and a separation distance that is small relative to a large epicentral distance, it is reasonable to assume that their motions will differ mainly due to the differences in $S(f)$, while their $P(f)$ can be assumed to be nearly the same. This reasoning has evolved into a framework for most theoretical and empirical studies of the effects of site conditions on the amplitudes of strong ground motion [6,67].

In Eq. (1), $S(f)$ models the site effects in general and can represent the geological site effects, the soil site effects, both of those together, the surface topography, and it may even include other site characteristics that may be relevant. In this paper, we discuss the role of $S(f)$ only when it represents the geological site effects, soil site effects, or both of these together, and we do not consider examples of any other site dependence.

2.1. Geological site conditions

Considering the size of geological inhomogeneities, the distances traveled by strong-motion waves, and the wavelengths associated with the frequencies of interest in earthquake engineering (0.05–50 Hz), it is clear that the local geologic conditions play a prominent role in determining the local site amplifications [68–73].

In this paper, we use “geological site conditions” to represent the binary view of the site conditions, determined from geological

maps ($s=0$ for sites on sediments, and $s=2$ for sites on the basement rock). Trifunac and Brady [74] show examples of how the geological site descriptions can be converted to $s=0$ or 2, and to $s=1$ for “in-between” sites, which are near the contact of sediments with basement rock, or which are in a complex setting that does not allow unequivocal and simple site description. Sites on sediments ($s=0$) can further be described by their thickness (h) above the basement rock [75,76]. The nature of the geological site conditions, as described by s and/or h , involves a scale that is measured in kilometres [67].

Before the advent of digital computers, analyses of the amplification of ground motion were performed by manually measuring the recorded peaks of instrument response. For example, Reid [2] found amplification of 1–2 for sandstone, 2–4 for sand, and 4–12 for man-made fill and marsh. For seismometer response to local earthquakes, with periods of the peaks in the range from 0.5 to 1 s, Gutenberg [9] analyzed recordings from 25 temporary stations on sediments and one reference station on basement rock. He found amplification of about 2–3 on deep sediments. Similar trends were later observed by Borchardt [77], Borchardt and Gibbs [78], and Campbell and Duke [79]. After digital data processing became possible, Trifunac and Brady [80] and Trifunac [68,81] extended this work to all peaks of strong ground motion and found excellent agreement with the results of Gutenberg [9] for periods longer than about 0.5 s and for peak velocities and peak displacements. However, they found a reversal of this trend for peak accelerations (i.e., for strong-motion amplitudes at high frequencies) and showed that the peak accelerations recorded on basement rock are comparable to or larger than the peaks recorded on sediments and on alluvium. The work of Trifunac and Brady [80] brought out the significance of the frequency-dependent nature in the amplification by local site effects.

2.2. Soil site conditions

Characterization of the soil site conditions involves a depth scale that originally extended to about 200 m (deep, cohesionless soils, as in [1]), but which in more recent studies has been reduced to only 30 m below the surface [82]. Because of the small thickness, soils can be expected to contribute mainly to the high-frequency, linear changes in the incident seismic waves, but because of their low stiffness and nonlinear behavior they can play a significant role in all frequencies of the observed motions. The soil site conditions introduced by Seed et al. [1] involve four groups: “rock” ($s_L=0$, for sites with a shear-wave velocity of less than 800 m/s and a thickness of less than 10 m), stiff soil sites ($s_L=1$, with a shear-wave velocity of less than 800 m/s and soil thickness of less than 75–100 m), deep soil sites ($s_L=2$, with a shear-wave velocity of less than 800 m/s and thickness of between 100 and 200 m), and soft-to-medium clay and sand ($s_L=3$) (where the notation $s_L = -1, 0, 1, 2, 3$ is as introduced and used by Trifunac [83] and Lee [84], and $s_L = -1$ is used in their regression analyses for sites with unknown soil-site conditions).

Categorical variables, which describe the shallow soil site conditions in terms of the average shear-wave velocity v_L in the top 30 m of soil, were first defined as: A for $v_L > 750$ m/s, B for $360 < v_L < 750$ m/s, C for $180 < v_L < 360$ m/s, and D for $v_L < 180$ m/s. With minor variations, these categorical variables continue to be refined as more data become available [82].

Trifunac [83] showed that the local soil and geologic site conditions must be considered simultaneously in the empirical scaling of strong-motion Fourier spectral amplitudes, and he presented a family of such scaling equations. Lee [84] extended this work to the scaling of pseudo relative velocity spectra. In

searching for the most stable equations, and in order to find the type of regression analysis that is most suitable for such scaling, they consider eight different models, two pairs for direct scaling in terms of the local geologic conditions modelled by the depth of sediments, and two pairs for scaling in terms of the simple geologic site conditions ($s=0, 1$, and 2). Each pair consisted of one set of equations for scaling in terms of earthquake magnitude and one set for scaling in terms of the site intensity. Corresponding to these four models, in which the simultaneous effects of both local soil and local geologic conditions were considered, a set of four other models with two-stage regression was also analyzed, in the first stage with respect to all scaling parameters, including the local geologic conditions, and then in the second stage with respect to the residuals in terms of the local soil conditions only. Some results of these regression analyses will be discussed later.

It should be noted here that both the derived scaling functions for site amplification in terms of the geological site parameters (s and h) and the soil site parameters (s_L), as well as the corresponding parameters in the site database, are correlated. This is to be expected because of the nature of the creation, transport, and deposition of soil materials. For the data set used by Trifunac [83], there were many (33%) deep-soil sites ($s_L=2$) over sediments ($s=0$ or $h > 0$) and 10% “rock”-soil sites ($s_L=0$) over basement rock ($s=2$, or $h=0$). There were, however, also many (27%) stiff-soil sites ($s_L=1$) over sediments ($s=0$ or $h > 0$) and 8% “rock”-soil sites ($s_L=0$) over intermediate geologic sites ($s=1$) [67]. Consequently, the use of regression models, which describe the site conditions in terms of only soil or geological site parameters, averages out the dependence upon the site parameter that is not used in the analysis. This leads to erroneous prediction of the amplification by local site conditions, and, using the distribution of the site conditions in the study by Trifunac [83] as an illustration, these erroneous predictions occur about 40% of the time. Yet, it is remarkable how many studies still continue to develop scaling equations using only the soil site classification variables (e.g., [85–88]), as if all strong-motion data have been recorded under identical geologic site conditions.

In the following, we discuss only the dependence of the empirical scaling equations on the s , h , s_L , and v_L (or A, B, C, and D) site parameters. A discussion of other site-specific parameters that have been considered in the analysis of the local site effects on the amplitudes of strong motion can be found in [30], and on the duration of strong ground motion in [89–93].

3. The regression of peak acceleration

3.1. Previous analyses

Comprehensive regression analyses of earthquake strong-motion parameters started to appear in the early 1970s. It was then suggested that the peaks of strong earthquake ground motion could be scaled as follows [68,74]:

$$\log \begin{Bmatrix} a_{\max} \\ v_{\max} \\ d_{\max} \end{Bmatrix} = M + \log_{10} A_0(R) - \log \begin{Bmatrix} a_0(M, \dots) \\ v_0(M, \dots) \\ d_0(M, \dots) \end{Bmatrix} \quad (2)$$

where a_{\max} , v_{\max} , and d_{\max} , respectively, are instrument- and baseline-corrected peak acceleration, velocity, and displacement amplitudes [33,94]; M is the earthquake magnitude; $\log_{10} A_0(R)$ is Richter's amplitude attenuation function [95] versus epicentral distance R , and $a_0(M, \dots)$, $v_0(M, \dots)$, and $d_0(M, \dots)$ are the magnitude site-dependent empirical (“correction”) scaling functions for acceleration, velocity, and displacement.

Trifunac [81] and Trifunac and Anderson [72,73] generalized Eq. (2) to apply for Fourier (FS) and pseudo relative velocity response (PSV) amplitude spectra at a set of discrete periods, T , as follows:

$$\log \left\{ \frac{FS(T)}{PSV(T)} \right\} = M + \log A_0(R) - \log \left\{ \frac{FS_0(M, \dots)}{PSV_0(M, \dots)} \right\} \quad (3)$$

where $FS(T)$ and $PSV(T)$ are the Fourier and response spectral amplitudes. The site dependence used in both Eqs. (2) and (3) was the geological site condition parameter, s .

In the late 1970s, Trifunac and Lee [75,76], introduced a more “refined” parameter to describe the local geology, namely the depth of sedimentary deposits, h . The new scaling equations became

$$\log \{FS(T) \text{ or } PSV\} = M + \log A_0(R) - b(T)M - c(T) - d(T)h - c(T)v - f(T)M^2 - g(T)R(T) \quad (4)$$

where v designates the horizontal ($v=0$) or vertical ($v=1$) components; R is the epicentral distance, and all other parameters are as defined above. The scaling functions $b(T)$ through $g(T)$ were determined by regression at 91 periods, T , between 0.04 and 15 s.

The term $\log A_0(R)$ was empirically determined for Southern California [95] and represents an average combination of geometric spreading, scattering, and inelastic attenuation at a frequency band around 1 Hz. The advantage in using the term $\log A_0(R)$ has been that it contains information on the average properties of wave propagation through the crust in Southern California, where most strong-motion data were recorded up to the early 1970s.

By the mid-1980s, the list of contributing earthquakes grew to 104 and included regions outside Southern California. Further, it was noted that the term $\log A_0(R)$ did not depend upon the magnitude or the earthquake source dimensions, or on the frequencies of the recorded waves. It was expected that the slope of the attenuation equations should be steeper for small-magnitude earthquakes and that for larger ones it would tend to flatten out with a smaller slope at small distances from the fault. To be able to explicitly consider such trends, Trifunac and Lee [96] developed the first generation of frequency-dependent attenuation functions of Fourier spectrum amplitudes. These were developed to model the trends of the available data and to have sufficient flexibility to include the dependence on magnitudes, source dimensions, focal depth, and frequencies of the wave motion. The Richter's attenuation function $\log A_0(R)$ was then replaced by

$$Att(\Delta, M, T) = \tilde{A}_0(T) \log_{10} \Delta \quad (5)$$

where $\tilde{A}_0(T)$ is an empirically determined function of period T , and $\Delta = \Delta(M, D, T)$ is the representative source-to-station distance for wave motions at period T from an earthquake with magnitude M at a site with hypocentral distance $D = (R^2 + H^2)^{1/2}$. R is epicentral distance, H is hypocentral depth (both in kilometres), and

$$\Delta = S \left(\ln \frac{R^2 + H^2 + S_0^2}{R^2 + H^2 + S_0^2} \right)^{1/2} \quad (6)$$

S_0 in Eq. (6) is the correlation radius of the source function and can be approximated by $S_0 \sim \beta T/2$, where β is the shear wave velocity in the source region [96,97]. H is the hypocentral depth of the source, and S , the “source dimension,” was approximated by a

straight line versus magnitude

$$S = \begin{cases} -25.34 + 8.51 M & \text{for } 3 \leq M \leq 7.25 \\ 0.2 & \text{for } M \leq 3 \end{cases} \quad (7)$$

For the analysis in this paper, the attenuation “coefficient” $\tilde{A}_0(T)$ in Eq. (5) will be determined for peak accelerations at one chosen period T , when the attenuation of strong-motion peak acceleration is determined for distances within about 100 km from the source. At distances exceeding this range [96,98,99], the strong-motion data are expected to consist primarily of surface waves. At these and larger distances, the recorded strong-motion amplitudes become small and consist of longer periods. This means that the strong-motion accelerographs will also cease to be triggered, especially for smaller-magnitude earthquakes. Consequently, at these and larger distances, the lack of recorded strong-motion data will not allow any reliable estimates of the attenuation functions. To describe approximately the attenuation at these large distances, Eq. (5) for peak acceleration will be modified. We will require that it should have slope of $-1/200$. The new attenuation function, with $b_0 = \tilde{A}_0(T)$ at $T = 0.1$ s for peak acceleration, will take the form

$$Att(\Delta, M, T)_{T=0.1} = \begin{cases} b_0 \log \Delta & \text{for } R \leq R_{\max} (\Delta \leq \Delta_{\max}) \\ b_0 \log \Delta_{\max} - (R - R_{\max})/200 & \text{for } R > R_{\max} (\Delta > \Delta_{\max}) \end{cases} \quad (8)$$

with Δ_{\max} being the representative source-to-station distance evaluated at $R = R_{\max}$. Eq. (8) shows that at distances $R > R_{\max}$ the attenuation is a linear function with slope $-1/200$. The slope of the attenuation for $R < R_{\max}$ depends upon the epicentral distance, R , the focal depth, H and the source dimension, S .

To determine the transition distance R_{\max} (much further out than the fault size S , i.e., $R = R_{\max} \gg S$) the following asymptotic approximation is used. For the case $R^2 + H^2 \gg S^2$, the representative distance Δ has the following asymptotic approximation:

$$\Delta \sim [(R^2 + H^2)/(1 - S_0^2/S^2)]^{1/2} \quad (9)$$

The slope of this attenuation function is

$$\frac{d}{dR} (b_0 \log_{10} \Delta) \sim \frac{b_0 (1 - S_0^2/S^2) R}{(R^2 + H^2) \ln 10} \quad (10)$$

which, when equated to a slope of $-1/200$, gives

$$R^2 + \gamma R + H^2 = 0 \quad (11)$$

a quadratic equation in R , with the coefficient γ given by

$$\gamma = \frac{200 b_0 (1 - S_0^2/S^2)}{\ln 10} \quad (12)$$

The solution, $R = R_{\max}$, is then given by

$$R_{\max} = 0.5(-\gamma + \sqrt{\gamma^2 - 4H^2}) \quad (13)$$

3.2. The regression equations: step 1

The regression of peak accelerations can be performed via a multi-step residue model, where in the first step the logarithm of peak acceleration, $\log_{10} a_{\max}$, is scaled in terms of earthquake magnitude, M ; local site geology, characterized in terms of the local geological site parameter, s , or depth of sediments, h ; and component direction, v . Two models were considered in the first step: the *magnitude-site model* and the *magnitude-depth model*.

(i) *Mag-site model*: the scaling equation takes the form

$$\log a_{\max} = \begin{cases} M + b_0 \log(\Delta/L) + b_1 M + b_2 s + b_3 v + b_4 + b_5 M^2 & \text{if } R \leq R_{\max} (\Delta \leq \Delta_{\max}) \\ M + b_0 \log(\Delta_{\max}/L) + b_1 M + b_2 s + b_3 v + b_4 + b_5 M^2 - (R - R_{\max})/200 & \text{if } R > R_{\max} (\Delta > \Delta_{\max}) \end{cases} \quad (14)$$

In this model, $\Delta = \Delta(D, M, T)$ is the representative “source-to-station” distance, and $L = L(M)$ is the rupture length of the earthquake fault. It is approximately described by $L = 0.01 \times 10^{0.5M}$ km [100,101]. Δ/L is thus a dimensionless representative distance. R_{\max} and Δ_{\max} are the epicentral and representative cutoff distances beyond which the attenuation of $\log_{10} a_{\max}$ will have a slope of $-1/200$, identical to Richter’s empirical attenuation law at large distances, and $S(M)$ is the size of the earthquake fault of magnitude M . $S(M)$ is a linear function of magnitude, such that [96]

$$S(3.0) = 0.20 \text{ km} \quad \text{and} \quad S(6.5) = 30.0 \text{ km} \quad (15)$$

(see Eq. (7)) and, for $M \geq 7.25$, $S(M) = S(7.25)$.

(ii) *Mag-depth model*: the scaling equation is

$$\log a_{\max} = \begin{cases} M + b_0 \log(\Delta/L) + b_1 M + b_2 h + b_3 v + b_4 + b_5 M^2 \\ M + b_0 \log(\Delta_{\max}/L) + b_1 M + b_2 h + b_3 v + b_4 + b_5 M^2 - (R - R_{\max})/200 \end{cases}$$

This model is identical to model (i) except that the local geology is now characterized by the depth of sediments, h , instead of by the site condition parameter s . In both models, Δ_{\max} is Δ evaluated at $R = R_{\max}$. For both models (i) and (ii), in definition of Δ , the correlation radius S_0 of the source functions will be taken equal to 0.1 km (for an example, see Appendix F in [102]).

4. Dependence of peak acceleration on local soil conditions

Step 1 of the regression analysis involves the local geology at the recording site characterized either by the local geological site-condition parameter, s ($s=0, 1$, or 2), or by the depth of sediments, h (in km). The second step of the regression will deal with the dependence of recorded peak acceleration on the local soil at the site. The local soil at the recording site (down to 100–200 m depth, [1]) has been characterized by local soil-site classification consisting of four groups: $s_L=0$ (“rock” soil), $s_L=1$ (stiff soil), $s_L=2$ (deep soil) and $s_L=3$ (deep cohesionless soil). In California, instrumented sites with $s_L=3$ are rare, so an insignificant number of records have been available to consider this type of site in any past or current regression analyses [67]. We mention this site classification here for completeness of this presentation, and we proceed with analysis for $s_L=0, 1$, and 2 only. In the regression analysis, the sites for which there is no information to assign the soil-site parameter s_L , are identified by $s_L = -1$. In addition, the average soil velocity, v_L (in km/s) in a surface “layer” 30 m deep, if measured, will also be used.

4.1. The regression equations: step 2a

The residues from the first step of regression are first calculated:

$$\varepsilon = \log a_{\max} - \log \hat{a}_{\max} \quad (17)$$

corresponding, at each site, to the difference between the actual $\log a_{\max}$ and the estimated value of $\log \hat{a}_{\max}$ using the regression Eq. (14) or Eq. (16) in step 1. These residues will then be fitted with models involving the soil parameters s_L or v_L separately. First, we consider the soil parameter, s_L , using categorical variables, representing the residual ε as

$$\varepsilon = b_7^{(-1)} S_L^{(-1)} + b_7^{(0)} S_L^{(0)} + b_7^{(1)} S_L^{(1)} + b_7^{(2)} S_L^{(2)} + b_7^{(3)} S_L^{(3)} \quad (18)$$

where $S_L^{(-1)}, S_L^{(0)}, S_L^{(1)}, S_L^{(2)}, S_L^{(3)}$ are categorical variables for the soil type s_L .

Each of these categorical variables, $S_L^{(i)}$ for $i = -1$ to 3 is defined by

$$S_L^{(i)} = \begin{cases} 1 & \text{if } s_L = i \\ 0 & \text{otherwise} \end{cases} \quad (19)$$

The category $s_L=3$ was considered for one specific site with about 10 recorded peak values. Until there is enough data in this category, the results for this soil category should be viewed only as an illustration of possible trends.

Analysis shows that the mean residues for categories 0 (“rock”) and 1 (stiff soil) are almost identical. In the following, these two categories will be assumed to have the same mean levels $\mu_0 = \mu_1$.

The residuals for case $s_L=3$ (deep, cohesionless sites) have a mean equal to ~ -0.66 , significantly different from the mean

$$\begin{cases} \text{if } R \leq R_{\max} \quad (\Delta \leq \Delta_{\max}) \\ \text{if } R > R_{\max} \quad (\Delta > \Delta_{\max}) \end{cases} \quad (16)$$

amplitudes of the residuals in other categories. Since the number of data points in this group is very small, it is not possible to make any definite conclusions about the dependence of peak acceleration on soil type in this category. However, the result is consistent with the expected trend of peak acceleration on soft soils, namely that the peak acceleration will be lower in very soft soil. This trend is in qualitative agreement with our previous work dealing with regression analyses of pseudo relative velocity spectra (PSV) amplitudes [84]. It was observed then that the spectral amplitudes for short periods ($T < 0.1$ s) are higher on “rock” and “stiff” soil than on “deep” soil sites.

The dependence of peak acceleration on average soil velocity v_L was studied next. Recall that the soil-type parameter, s_L , describes the soil stiffness in the top 100–200 m below the ground surface at the site. The average soil velocity, v_L , on the other hand, represents the average velocity of shear waves only in the top 30 m below surface.

4.2. The regression equations: step 2b

We start with the residues (after fitting the dependence on magnitude, distance, geologic site conditions, and soil type in step 2a), and consider the following regression:

$$\varepsilon = b_8^{(0)} + b_8^{(1)} v_L + b_8^{(2)} v_L^2 \quad (20)$$

Here the residue represents the difference between ε of Eq. (18) and the corresponding means μ_i , for the data in the soil type categories for $i = -1$ to 3 . It is fitted by a parabola versus v_L . The residues are in the range from -1 to $+1$ on the log scale, or in a range [0.1, 10.] on a linear scale [102]. The polynomial fitted versus v_L shows little to no difference from zero. This demonstrates that the dependence of peak acceleration on average soil velocity, v_L , is insignificant (the 95% confidence interval, mean $+1.96 \times$ standard deviation, would all include 0). The result is not in contradiction with the dependence of peak accelerations on soil type s_L , as described above. It simply means that the average soil velocity—only in the top 30 m below the surface—is not an important parameter, which influences the amplitudes of the recorded peak accelerations. If the average soil-velocity parameter, v_L , were to show some significance in determining the amplitudes of peak acceleration, perhaps we would need to measure its average value at each site to some greater depth, or, for example, to the depths associated with the definition of the values of the s_L parameter.

The residues from the *mag-depth model* in step 1 can also be used to study the dependence of peak acceleration on soil type s_L and average soil velocity v_L . Again, analysis shows that the

dependence of peak acceleration amplitudes on average soil velocity v_L is not significant.

In conclusion, both the residues from the mag-site and mag-depth models show a dependence of peak acceleration on soil type s_L but no dependence on average soil velocity v_L .

4.3. Soil type s_L versus soil velocity v_L

Steps 2a and 2b of the regression of peak accelerations with local soil type parameter s_L and average soil velocity v_L at the site, as performed above, show that the soil-type parameter s_L is stable and consistent with many previously analyzed trends, while the soil-velocity parameter v_L is not significant. As already noted, this could be due to the fact that s_L represents the soil profile up to about 200 m below the surface, whereas the average soil-velocity parameter v_L represents only the average soil velocity in the top 30 m below the surface.

It could be that the significance of average soil velocity v_L is overshadowed by that of soil type s_L because the soil type s_L was fitted in the first step of regression (step 2a), while the soil velocity v_L was fitted in the second step. To investigate this possibility, these two steps of regression were repeated, but this time in a reverse order. Starting with the same residues as in Eq. (17), we first fitted those by a parabola using the soil velocity v_L in the first step, as in Eq. (20), and then the resulting residues from this first step were fitted with the local soil type s_L in the second step using the same categorical variables as in Eq. (18).

We found again that the fitted parabola is not much different from zero, confirming the previous inference that the average soil-velocity parameter, as used here, is not significant. The trend observed in the second step is similar to what was previously seen when the local soil type was fitted before the average soil velocity. This is not surprising because the amplitude of the parabolic fit of v_L is not very different from zero.

When we examine the residues versus the average soil velocity v_L versus the local soil type s_L , respectively, in the first and second steps of regression for the mag-depth model, the same conclusion can be drawn again: the average soil-velocity parameter is insignificant, and the local soil-type parameter has similar behavior as before, irrespective of the order in which these two are fitted to the residuals.

4.4. Soil type parameter, s_L , versus soil-velocity-type parameter S_T

The analyses in the previous section suggest that the characterization of the local soil in terms of the soil-type parameter s_L is more significant than the characterization by average soil velocity v_L measured for the top 30 m below the surface at the site. This section presents a different statistical evaluation of the significance of the soil type s_L versus the average soil velocity v_L . Because the s_L parameter used here is a discrete variable ($s_L = -1, 0, 1, 2$, and 3) and the v_L parameter is a continuous variable ($0 \leq v_L < 1.5$; v_L in km/s), a convenient way to measure and compare their significance is to discretize the velocity v_L parameter. Another good reason for discretizing the v_L parameter is to reduce the error resulting from the uncertainties involved in measuring the soil velocity v_L . In discretizing, the data have been divided into the following five groups:

Group	Velocity (km/s)
?	Unknown
A	$0.75 < v_L$
B	$0.36 < v_L < 0.75$
C	$0.18 < v_L < 0.36$
D	$v_L < 0.18$

Thus, every site in the database is classified into one of these velocity groups, just as each site is classified into one of the five soil-type groups ($s_L = -1$ to 3). The regression analyses of the previous section can now be repeated, in terms of

$$\varepsilon = \sum b^i S_L^i \quad (21)$$

and

$$\varepsilon = \sum b^i V_L^i \quad (22)$$

with $S_L^i <$ and V_L^i representing the categorical variables for the soil type s_L and velocity type v_L parameters. The regressions are performed for both the mag-site model (i) and the mag-depth model (ii), and in 2 steps, with s_L in the first step and v_L in the second step or vice versa.

The fitted coefficients $\mu_i = \hat{b}^i$ resulting from regression with either Eq. (21) or (22) represent the mean values of the residues in that particular class. The corresponding standard deviation σ_i can also be calculated. To examine the relative significance of the soil-type versus velocity-type classifications, the following hypothesis can then be tested:

H0. $\mu_i = \mu_j$ —i.e., there is essentially no difference between the data in categories i and j .

H1. $\mu_i \neq \mu_j$ —i.e., there is significant difference between the data in categories i and j .

To test the hypothesis, the student t -statistic is used, for data in categories i and j . We define

$$t_{ij} = \frac{\mu_i - \mu_j}{\sigma_{ij} \sqrt{1/N_i + 1/N_j}} \quad (23)$$

and

$$\sigma_{ij} = \sqrt{\frac{N_i \sigma_i^2 + N_j \sigma_j^2}{N_i + N_j - 2}} \quad (24)$$

With μ_i, μ_j representing the means of the residues in categories i and j , σ_i, σ_j representing the standard deviations of the residues in categories i and j , and N_i, N_j being the number of samples in categories i and j .

On the basis of a two-tailed test at a 0.01 level of significance or with a 99% level of confidence, hypothesis H_0 would be rejected and H_1 accepted if

$$|t_{ij}| > t_{0.995} \quad (25)$$

for $(N_i + N_j - 2)$ degrees of freedom. Similarly, H_0 would be rejected at the 0.05 level of significance or with a 95% level of confidence if

$$|t_{ij}| > t_{0.975} \quad (26)$$

for $(N_i + N_j - 2)$ degrees of freedom. Similarly, H_0 would be rejected at the 99% and at 95% levels of confidence for large data sets with $(N_i + N_j - 2) > 120$, when $|t_{ij}|$ is larger than

$$t_{0.995} = 2.58 \text{ and } t_{0.975} = 1.96 \quad (27)$$

To test the significance of the soil-type and velocity-type classifications, the hypothesis H_0 versus H_1 is tested using the student t -statistic of Eqs. (23)–(28) is the matrix of the t_{ij} statistics for the soil-type classification s_L :

$$(t_{ij}) = \begin{matrix} \begin{matrix} 1^{\text{st}} \text{ step} & s_L = -1 & 0 & 1 & 2 & 3 \end{matrix} \\ \begin{matrix} s_L = -1 \\ 0 \\ 1 \\ 2 \\ 3 \end{matrix} \begin{bmatrix} - & & 2.94 & -1.09 & 7.91 \\ -2.59 & - & -0.15 & -2.89 & 6.68 \\ -2.94 & 0.15 & - & -3.30 & 7.34 \\ 1.09 & 2.89 & 3.30 & - & 6.71 \\ -7.91 & -6.68 & -7.34 & -6.71 & - \end{bmatrix} \end{matrix} \quad (28)$$

$$\begin{array}{c} \text{2nd Step } S_T = ? \\ \begin{array}{ccccc} A & B & C & D \\ (t_{ij}) = \begin{bmatrix} - & 1.33 & -1.62 & -1.68 & 0.60 \\ -1.33 & - & -2.56 & -2.52 & -1.04 \\ -1.62 & 2.56 & - & -0.04 & -0.11 \\ 1.68 & 2.52 & 0.04 & - & -0.10 \\ -0.60 & 1.04 & 0.11 & -0.10 & - \end{bmatrix} \end{array} \end{array} \begin{array}{c} S_T = ? \\ A \\ B \\ C \\ D \end{array} \quad (29)$$

The t_{ij} matrices in both Eqs. (28) and (29) are anti-symmetric, and only the off-diagonal elements are defined. Recall from Eq. (27) that hypothesis H_0 can be rejected at the 95% level of confidence if $|t_{ij}| > 1.96$. Inspection of the t_{ij} matrix in Eq. (28) for soil type shows that except for soil types 0 and 1 (“rock” soil and “stiff” soil), with $|t_{01}| = |t_{10}| = 0.15$ (and types—1 and 2), the pairs of all other categories have $t_{ij}'s > 2$, or there is a 95% or higher level of confidence that different soil types indeed have different means. Thus, the soil type classification, s_L , divides the data into categories with significantly different means. The fact that $s_L = 0$ and 1 show little difference is consistent with the physical properties that sites with “rock” and “stiff” soil have insignificant differences in peak amplitudes.

Inspection of the (t_{ij}) matrix in Eq. (29) for average soil velocity, on the other hand, shows that except for the row and the column corresponding to velocity type A ($v_L > 0.75$ km/s), all the t_{ij} statistics are significantly less than 1, meaning that all categories except type A have insignificantly different means.

The residues are next fitted with soil type and velocity type in reverse order. The residues from Eq. (22) will be considered in the first step, followed by those for soil type (Eq. (21)) in the second step. Eqs. (30) and (31) give the corresponding (t_{ij}) matrices:

$$\begin{array}{c} \text{1st step } S_T = ? \\ \begin{array}{ccccc} A & B & C & D \\ (t_{ij}) = \begin{bmatrix} - & 2.46 & 0.27 & -0.34 & -0.75 \\ -2.46 & - & -2.19 & -2.55 & -1.60 \\ -0.27 & 2.19 & - & -0.63 & 0.79 \\ 0.34 & 2.55 & 0.63 & - & -0.57 \\ 0.75 & 1.60 & 0.79 & -0.57 & - \end{bmatrix} \end{array} \end{array} \begin{array}{c} S_T = ? \\ A \\ B \\ C \\ D \end{array} \quad (30)$$

$$\begin{array}{c} \text{2nd step } s_L = -1 \quad 0 \quad 1 \quad 2 \quad 3 \\ (t_{ij}) = \begin{bmatrix} - & 1.87 & 3.56 & -0.36 & 8.12 \\ -1.87 & - & 1.03 & -1.73 & 6.95 \\ -3.56 & -1.03 & - & -3.07 & 7.40 \\ 0.36 & 1.73 & 3.07 & - & 6.68 \\ -8.12 & -6.95 & -7.40 & -6.68 & - \end{bmatrix} \end{array} \begin{array}{c} s_L = -1 \\ 0 \\ 1 \\ 2 \\ 3 \end{array} \quad (31)$$

Inspection of the (t_{ij}) matrix for velocity type (V_T) in the first step (Eq. (30)) shows that 14 of the 20 off-diagonal elements are less than 2, implying that the peak accelerations for sites with different velocity-type categories do not show significant differences. The (t_{ij}) matrix for soil type (s_L) in the second step (Eq. (31)), on the other hand, shows that 12 of the 20 off-diagonal elements are above 2 (or 8 of the 20 are below 2), showing that the data in different soil categories, s_L , do display more significant differences in the amplitudes of recorded peak accelerations.

Eqs. (32)–(35) give the corresponding (t_{ij}) matrices of soil-type and velocity-type categories, for the *mag-depth model*, as

Eqs. (28)–(31) did for the *mag-site model*:

$$\begin{array}{c} \text{1st step } s_L = -1 \quad 0 \quad 1 \quad 2 \quad 3 \\ (t_{ij}) = \begin{bmatrix} - & 1.48 & 2.19 & -0.86 & 7.70 \\ -1.48 & - & 0.39 & -2.00 & 6.81 \\ -2.19 & -0.39 & - & -2.73 & 7.25 \\ 0.86 & 2.00 & 2.73 & - & 6.59 \\ -7.70 & -6.81 & -7.25 & -6.59 & - \end{bmatrix} \end{array} \begin{array}{c} s_L = -1 \\ 0 \\ 1 \\ 2 \\ 3 \end{array} \quad (32)$$

$$\begin{array}{c} \text{2nd step } S_T = ? \\ \begin{array}{ccccc} A & B & C & D \\ (t_{ij}) = \begin{bmatrix} - & 1.65 & -1.19 & -0.94 & -0.36 \\ -1.65 & - & -2.66 & -2.40 & -0.94 \\ -1.19 & 2.66 & - & -0.30 & 0.02 \\ 0.94 & 2.40 & 0.30 & - & -0.06 \\ 0.36 & 0.94 & -0.02 & -0.06 & - \end{bmatrix} \end{array} \end{array} \begin{array}{c} S_T = ? \\ A \\ B \\ C \\ D \end{array} \quad (33)$$

$$\begin{array}{c} \text{1st step } S_T = ? \\ \begin{array}{ccccc} A & B & C & D \\ (t_{ij}) = \begin{bmatrix} - & 2.48 & 0.14 & -0.02 & -0.48 \\ -2.48 & - & -2.35 & -2.41 & -1.35 \\ -0.14 & 2.35 & - & -0.17 & 0.50 \\ 0.02 & 2.41 & 0.17 & - & -0.41 \\ 0.48 & 1.35 & 0.50 & -0.41 & - \end{bmatrix} \end{array} \end{array} \begin{array}{c} S_T = ? \\ A \\ B \\ C \\ D \end{array} \quad (34)$$

$$\begin{array}{c} \text{2nd step } s_L = -1 \quad 0 \quad 1 \quad 2 \quad 3 \\ (t_{ij}) = \begin{bmatrix} - & 0.82 & 2.70 & -0.36 & 7.88 \\ -0.82 & - & 1.50 & -1.00 & 7.07 \\ -2.70 & -1.50 & - & -2.65 & 7.27 \\ 0.36 & 1.00 & 2.65 & - & 6.56 \\ -7.88 & -7.07 & -7.27 & -6.56 & - \end{bmatrix} \end{array} \begin{array}{c} s_L = -1 \\ 0 \\ 1 \\ 2 \\ 3 \end{array} \quad (35)$$

Inspection of the matrices (Eqs. (32)–(35)) for the *mag-depth model* shows that the results are consistent with those of the *mag-site model*.

In summary, the (t_{ij}) student t-statistics suggests that the soil type classification is more significant than the velocity type classification in influencing the amplitudes of recorded peak ground acceleration.

5. Discussion and conclusions

We examined the relative significance of two different soil-site variables that are used in empirical equations aiming to predict amplification of strong earthquake motion: (1) of soil site classification s_L and (2) of the average soil velocity, v_L , in the top 30 m of soil. The regressions of peak accelerations with local soil type parameter s_L and average soil velocity v_L at the site show that the soil type parameter s_L is stable and consistent with many previously analyzed trends, while the soil velocity parameter v_L is not significant. We pointed out that the local soil type parameter (e.g., $s_L = 2$) represents the average soil profile up to 200 m below the surface, whereas the average soil velocity parameter v_L represents only the average soil velocity in the top 30 m below the surface. If the average soil velocity parameter, v_L , were to show some significance in determining the amplitudes of peak acceleration, perhaps we would need to measure its average value at each site to greater depths, or, for example, to the depths associated with the definition of the values of the s_L parameter.

In the second part of the analysis, we discretized the data on v_L into four groups (A, B, C, and D) and studied the significance of the

differences of the means in those groups. We performed the same analysis for the four groups of s_L parameters. The results of this analysis conformed that s_L is a significant site parameter, while v_L is not.

In a recent paper, Castellaro et al. [103], not aware of our work in the mid-1990s [102], found that “in spite of its almost universal adoption as a key parameter in seismic site classification, v_L appears a weak proxy to seismic amplification”. Their analysis, based on a different data set and using a different method of analysis, arrived at essentially the same conclusion as we did in 1995, and as described again in this paper.

Acknowledgements

We are indebted to two anonymous reviewers whose detailed comments and suggestions lead to significant improvements of our paper.

References

- [1] Seed HB, Ugas C, Lysmer J. Site-dependent spectra for earthquake-resistant design. *Bull Seismol Soc Am* 1976;66:221–43.
- [2] Reid HF, 1910. The California earthquake of April 18, 1906, in *The Mechanics of the earthquake*, vol. 2. Report of the State Earthquake Investigation Commission, Carnegie Institute of Washington, Publication 87, Washington, DC.
- [3] Duke CM. Bibliography of effects of soil conditions on earthquake damage. Berkeley, CA: Earthquake Engineering Research Institute; 1958.
- [4] Freeman JR. Earthquake damage and earthquake insurance. New York: McGraw-Hill; 1932.
- [5] Coulter HW, Waldron HH, Devine JF. Seismic and geologic siting considerations for nuclear facilities. In: *Proceedings of the fifth world conference on earthquake engineering*, Rome, Italy; 1973.
- [6] Kanai K. *Engineering seismology*. Tokyo: University of Tokyo Press; 1983.
- [7] Trifunac MD. Recording strong earthquake motion—instruments, recording strategies and data processing. Los Angeles, California: Department of Civil Engineering, University of Southern California; 2007. Report CE 07-03.
- [8] Trifunac MD. 75th anniversary of strong motion observation—a historical review. *Soil Dyn Earthquake Eng* 2009;29(4):591–606.
- [9] Gutenberg B. Effects of ground on earthquake motion. *Bull Seismol Soc Am* 1957;47:221–50.
- [10] Ambraseys NN, Simpson KA, Bommer JJ. Prediction of horizontal response spectra in Europe. *Earthquake Eng Struct Dyn* 1996;25:371–400.
- [11] Lee VW. Empirical scaling and regression methods for earthquake strong-motion spectra—a review. *ISER J* 2007;44(1):39–69.
- [12] Trifunac MD, Hao TY, Todorovska MI. On reoccurrence of site specific response. *Soil Dyn Earthquake Eng* 1999;18(8):569–92.
- [13] Trifunac MD, Ivanović SS. Reoccurrence of site specific response in former Yugoslavia—Part I: Montenegro. *Soil Dyn Earthquake Eng* 2003;23(8):637–61.
- [14] Trifunac MD, Ivanović SS. Reoccurrence of site specific response in former Yugoslavia—Part II: Friuli, Banja Luka, and Kopaonik. *Soil Dyn Earthquake Eng* 2003;23(8):663–81.
- [15] Trifunac MD, Lee VW. Peak surface strains during strong earthquake motion. *Soil Dyn Earthquake Eng* 1996;15(5):311–9.
- [16] Trifunac MD, Novikova EI, 1995. State of the art review on strong motion duration. In: *Proceedings of the 10th European conference on earthquake engineering*, August 28–September 2, 1994, vol. 1, Vienna, Austria. Rotterdam: A.A. Balkema; p. 131–40.
- [17] Trifunac MD. Q and high frequency strong motion spectra. *Soil Dyn Earthquake Eng* 1994;13(3):149–61.
- [18] Trifunac MD, 2005. Power design method. In: *Proceedings of the earthquake engineering in the 21st century to mark 40th anniversary of IZILIS—Skopje*, Key-note lecture, August 28–September 1, 2005, Skopje and Ohrid, Macedonia.
- [19] Todorovska MI, Trifunac MD. Discussion of “The role of earthquake hazard maps in loss estimation: A study of the Northridge Earthquake,” by R.B. Olshansky. *Earthquake Spectra* 1998;14(3):557–63.
- [20] Trifunac MD, Todorovska MI. Reduction of structural damage by nonlinear soil response. *J Struct Eng ASCE* 1999;125(1):89–97.
- [21] Trifunac MD, Todorovska MI. Nonlinear soil response as a natural passive isolation mechanism—the 1994 Northridge, California earthquake. *Soil Dyn Earthquake Eng* 1998;17(1):41–51.
- [22] Trifunac MD, Todorovska MI. Damage distribution during the 1994 Northridge, California, earthquake in relation to generalized categories of surficial geology. *Soil Dyn Earthquake Eng* 1998;17(4):239–53.
- [23] Trifunac MD, Todorovska MI, 1998. Amplification of strong ground motion and damage patterns during the 1994 Northridge, California, earthquake. In: Dakoulas P, Yegian M, Holta R, editors. *Proceedings of the third ASCE specialty conference on geotechnical earthquake engineering and soil dynamics*, 3–6 August 1998, Seattle, Washington; also in *Geotechnology Earthquake Engineering and Soil Dynamics III*, vols. 1 and 2, book series: geotechnical special publication, vol. 75(1). Reston, Virginia: ASCE; 1998. p. 714–25.
- [24] Trifunac MD, Todorovska MI, Ivanović SS. A note on distribution of uncorrected peak ground accelerations during the Northridge, California, earthquake of 17 January 1994. *Soil Dyn Earthquake Eng* 1994;13(3):187–96.
- [25] Aptikav F, Erteleva O. Standing waves and macroseismic field: empirical and theoretical evidences. In: *First European conference on earthquake engineering and seismology*, Paper 1291, CD ID 581, 2006.
- [26] Wong HL, Trifunac MD. Scattering of plane SH-waves by a semi-elliptical canyon. *Int J Earthquake Eng Struct Dyn* 1974;3(2):157–69.
- [27] Wong HL, Trifunac MD. Surface motion of a semi-elliptical alluvial valley for incident plane SH-waves. *Bull Seismol Soc Am* 1974;64(5):1389–408.
- [28] Todorovska MI, Trifunac MD. Amplitudes, polarity and time of peaks of strong ground motion during the 1994 Northridge, California Earthquake. *Soil Dyn Earthquake Eng* 1997;16(4):235–58.
- [29] Todorovska MI, Trifunac MD. Distribution of pseudo spectral velocity during Northridge, California earthquake of 17 January, 1994. *Soil Dyn Earthquake Eng* 1997;16(3):173–92.
- [30] Trifunac MD. The nature of site response during earthquakes. In: Schantz T, Iankov R, editors. *Coupled site and soil-structure interaction effects with applications to seismic risk mitigation, NATO science for peace and security series C: environmental security*. Springer Science+Business Media, B.V.; 2009. p. 3–31.
- [31] Wong HL, Trifunac MD, Westermo B. Effects of surface and subsurface irregularities on the amplitudes of monochromatic waves. *Bull Seismol Soc Am* 1977;67(2):353–68.
- [32] Lee VW, Trifunac MD. Response of tunnels to incident SH-waves. *ASCE, EMD* 1979;105(4):643–59.
- [33] Trifunac MD. A note on correction of strong-motion accelerograms for instrument response. *Bull Seismol Soc Am* 1972;62(1):401–9.
- [34] Wong HL, Trifunac MD. Two-dimensional, antiplane, building-soil-building interaction for two or more buildings and for incident plane SH-waves. *Bull Seismol Soc Am* 1975;65:1863–85.
- [35] Trifunac MD, Ivanović SS, Todorovska MI, Novikova EI, Gladkov AA. Experimental evidence for flexibility of a building foundation supported by concrete friction piles. *Soil Dyn Earthquake Eng* 1999;18(3):169–87.
- [36] Trifunac MD, Ivanović SS, Todorovska MI. Apparent periods of a building I: Fourier analysis. *J Struct Eng ASCE* 2001;127(5):517–26.
- [37] Trifunac MD, Ivanović SS, Todorovska MI. Apparent periods of a building II: time–frequency analysis. *J Struct Eng, ASCE* 2001;127(5):527–37.
- [38] Luco JE, Trifunac MD, Wong HL. On the apparent changes in dynamic behavior of a nine-story reinforced concrete building. *Bull Seismol Soc Am* 1987;77(6):1961–83.
- [39] Aptikav F. Review of empirical scaling of strong motion for seismic hazard analyses. In: Trifunac MD, editor. *Selected topics in earthquake engineering—from earthquake source to seismic design and hazard mitigation*. Banja Luka, Republic of Srpska: ZIBL; 2009. p. 37–54. [Chapter 2].
- [40] Espinosa AF. Attenuation of strong horizontal ground acceleration in the Western United States and their relation to M_L . *Bull Seismol Soc Am* 1980;70(2):583–616.
- [41] Hanks T, Johnson DA. Geophysical assessment of peak acceleration. *Bull Seismol Soc Am* 1976;66(3):959–68.
- [42] Herrmann RB, 1977. Earthquake generated SH wave in the near-field and near-regional field, Paper S-77-12, US Army Engineering, Waterways Exp. Station, C.E., Vicksburg, Miss.
- [43] Jalali RS, Trifunac MD. Response spectra for near-source, differential and rotational strong motion. *Bull Seismol Soc Am* 2009;99(2B):1404–15.
- [44] Trifunac MD, Todorovska MI, Ivanović SS. Peak velocities, and peak surface strains during Northridge, California, earthquake of 17 January 1994. *Soil Dyn Earthquake Eng* 1996;15(5):301–10.
- [45] Joyner WB, Boore DM. Peak horizontal acceleration and velocity from strong motion records including records from the 1979 Imperial Valley, California, earthquake. *Bull Seismol Soc Am* 1981;71(6):2011–58.
- [46] Ghiaruttini C, Crosilla F, Siro L. Some maximized acceleration analysis of the 1976 Friuli earthquakes. *Boll Geof Teor Appl* 1979;XXI:3–52.
- [47] Ghiaruttini C, Siro L. The correlation of peak ground horizontal acceleration with magnitude, distance, and seismic intensity for Friuli and Ancona, Italy, an Alpidic belt. *Bull Seismol Soc Am* 1981;71(6):1993–2009.
- [48] Duke CM, Bore DM, Porcell R, 1972. Effects of site classification and distance on instrumental indices in the San Fernando earthquake, Rpt. UCLA-ENG-7247, Los Angeles, CA.
- [49] Trifunac MD, Todorovska MI. Nonlinear soil response—1994 Northridge California, earthquake. *J Geotech Eng ASCE* 1996;122(9):725–35.
- [50] Trifunac MD, Todorovska MI. Can aftershock studies predict site amplification? Northridge, CA, earthquake of 17 January, 1994 *Soil Dyn Earthquake Eng* 2000;19(4):233–51.
- [51] Trifunac MD. Dependence of Fourier spectrum amplitudes of recorded strong earthquake accelerations on magnitude, local soil conditions and on depth of sediments. *Int J Earthquake Eng Struct Dyn* 1989;18(7):999–1016.
- [52] Trifunac MD. A method for synthesizing realistic strong ground motion. *Bull Seismol Soc Am* 1971;61(6):1739–53.

- [53] Wong HL, Trifunac MD. Generation of artificial strong motion accelerograms. *Int J Earthquake Eng Struct Dyn* 1979;7(6):509–27.
- [54] Todorovska MI, Trifunac MD. The system damping, the system frequency and the system response peak amplitudes during in-plane building–soil interaction. *Earthquake Eng Struct Dyn* 1992;21(2):127–44.
- [55] Trifunac MD. Rotations in structural response. *Bull Seismol Soc Am* 2009;99(2B):968–79.
- [56] Udawadia FE, Trifunac MD. Characterization of response spectra through the statistics of oscillator response. *Bull Seismol Soc Am* 1974;64(1):205–19.
- [57] Trifunac MD. Empirical criteria for liquefaction in sands via standard penetration tests and seismic wave energy. *Soil Dyn Earthquake Eng* 1995;14(6):419–26.
- [58] Todorovska MI, Trifunac MD. Antiplane earthquake waves in long structures. *ASCE, EMD* 1989;115(2):2687–708.
- [59] Todorovska MI, Trifunac MD. Propagation of earthquake waves in buildings with soft first floor. *ASCE, EMD* 1990;116(4):892–900.
- [60] Todorovska MI, Trifunac MD. Note on excitation of long structures by ground waves. *ASCE, EMD* 1990;116(4):952–64.
- [61] Trifunac MD, Todorovska MI. Response spectra and differential motion of columns. *Earthquake Eng Struct Dyn* 1997;26(2):251–68.
- [62] Earthquake Engineering Research Institute, 1995. Northridge earthquake of January 17, 1994. Reconnaissance Rep., *Earthquake Spectra*, Suppl. C to vol. 11, vol. 1.
- [63] Trifunac MD, Todorovska MI. Northridge, California, earthquake of 17 January 1994: density of pipe breaks and surface strains. *Soil Dyn Earthquake Eng* 1997;16(3):193–207.
- [64] Trifunac MD, Todorovska MI. Northridge, California, earthquake of 1994: density of red-tagged buildings versus peak horizontal velocity and intensity of shaking. *Soil Dyn Earthquake Eng* 1997;16(3):209–22.
- [65] Haskell NA. Elastic displacements in the near-field of a propagating fault. *Bull Seismol Soc Am* 1969;59:865–908.
- [66] Trifunac MD. A three-dimensional dislocation model for the San Fernando, California, earthquake of 9 February 1971. *Bull Seismol Soc Am* 1974;64:149–72.
- [67] Trifunac MD. How to model amplification of strong earthquake ground motions by local soil and geologic site conditions. *Earthquake Eng Struct Dyn* 1990;19(6):833–46.
- [68] Trifunac MD. Preliminary analysis of the peaks of strong earthquake ground motion dependence of peaks on earthquake magnitude, epicentral distance and recording site conditions. *Bull Seismol Soc Am* 1976;66:189–219.
- [69] Trifunac MD. Preliminary empirical model for scaling Fourier amplitude spectra of strong motion acceleration in terms of modified Mercalli intensity and geologic site conditions. *Earthquake Eng Struct Dyn* 1979;7:63–74.
- [70] Trifunac MD. Response spectra of earthquake ground motion. *J Eng Mech Div ASCE* 1978;104:1081–97.
- [71] Trifunac MD, Anderson JG. Preliminary empirical models for scaling absolute acceleration spectra. Los Angeles, CA: Department of Civil Engineering, University of Southern California; 1977. Report no. 77–03.
- [72] Trifunac MD, Anderson JG. Preliminary empirical models for scaling pseudo relative velocity spectra. Los Angeles, CA: Department of Civil Engineering, University of Southern California; 1978. Report no. 78–04.
- [73] Trifunac MD, Anderson JG. Preliminary models for scaling relative velocity spectra. Los Angeles, CA: Department of Civil Engineering, University of Southern California; 1978. Report no. 78–05.
- [74] Trifunac MD, Brady AG. On the correlation of seismic intensity scales with the peaks of recorded strong ground motion. *Bull Seismol Soc Am* 1975;65:139–62.
- [75] Trifunac MD, Lee VW. Dependence of the Fourier amplitude spectra of strong motion acceleration on the depth of sedimentary deposits. Los Angeles, CA: Department of Civil Engineering, University of Southern California; 1978. Report no. 78–14.
- [76] Trifunac MD, Lee VW. Dependence of the pseudo relative velocity spectra of strong motion acceleration on the depth of sedimentary deposits. Los Angeles, CA: Department of Civil Engineering, University of Southern California; 1979. Report 79–02.
- [77] Borchardt RD. Effects of local geology on ground motion near San Francisco Bay. *Bull Seismol Soc Am* 1970;60:29–61.
- [78] Borchardt RD, Gibbs JF. Effects of local geological conditions in the San Francisco Bay region on ground motions and intensities of the 1906 earthquake. *Bull Seismol Soc Am* 1976;66:467–500.
- [79] Campbell K, Duke CM. Bedrock intensity attenuation and site factors from San Fernando earthquake records. *Bull Seismol Soc Am* 1974;64:173–85.
- [80] Trifunac MD, Brady AG. Correlations of peak acceleration, velocity and displacement with earthquake magnitude, epicentral distance and site conditions. *Int J Earthquake Eng Struct Dyn* 1976;4(5):455–71.
- [81] Trifunac MD. Preliminary empirical model for scaling Fourier amplitude spectra of strong ground acceleration in terms of earthquake magnitude, source to station distance and recording site conditions. *Bull Seismol Soc Am* 1976;66:1343–73.
- [82] Chiou B, Darragh R, Gregor N, Silva W. NGA project strong-motion database. *Earthquake Spectra* 2008;24(1):23–44.
- [83] Trifunac MD. Influence of local soil and geologic site conditions on Fourier spectrum amplitudes of recorded strong motion accelerations Los Angeles, CA: Department of Civil Engineering, University of Southern California; . Report no. CE 87–04.
- [84] Lee VW. Influence of local soil and geologic site conditions on pseudo relative velocity response spectrum amplitudes of recorded strong motion accelerations. Los Angeles, CA: Department of Civil Engineering, University of Southern California; 1987. Report no. CE 87–06.
- [85] Abrahamson NA, Silva WJ. Empirical response spectral attenuation relations for shallow crustal earthquakes. *Seismol Res Lett* 1997;68(1):94–127.
- [86] Ambraseys NN, Douglas J, Sarma SK, Smit PM. Equations for the estimation of strong ground motions from shallow crustal earthquakes using data from Europe and the Middle east: horizontal peak ground acceleration and spectral acceleration. *Bull Earthquake Eng* 2005;3:1–53.
- [87] Ambraseys NN, Douglas J, Sarma SK, Smit PM. Equations for the estimation of strong ground motions from shallow crustal earthquakes using data from Europe and the Middle East: vertical peak ground acceleration and spectral acceleration. *Bull Earthquake Eng* 2005;3:55–73.
- [88] Boore DM, Joyner WB, Fumal T. Equations for estimating horizontal response spectra and peak acceleration from western North American earthquakes: a summary of recent work. *Seismol Res Lett* 1997;68(1):128–53.
- [89] Novikova EI, Trifunac MD. Modified Mercalli intensity and the geometry of the sedimentary basin as the scaling parameters of the frequency dependent duration of strong ground motion. *Soil Dyn Earthquake Eng* 1993;12(4):209–25.
- [90] Novikova EI, Trifunac MD. Duration of strong earthquake ground motion: physical basis and empirical equations. Los Angeles, CA: Department of Civil Engineering, University of Southern California; 1993. Report no. CE 93–02.
- [91] Novikova EI, Trifunac MD. Duration of strong ground motion in terms of earthquake magnitude epicentral distance, site conditions and site geometry. *Earthquake Eng Struct Dyn* 1994;23(6):1023–43.
- [92] Novikova EI, Trifunac MD. Influence of geometry of sedimentary basins on the frequency dependent duration of strong ground motion. *Earthquake Eng Vib* 1994;14(2):7–44.
- [93] Novikova EI, Trifunac MD. Frequency dependent duration of strong earthquake ground motion: updated empirical equations. Los Angeles, CA: Department of Civil Engineering University of Southern California; 1995. Report no. CE 95–01.
- [94] Trifunac MD. Zero baseline correction of strong-motion accelerograms. *Bull Seismol Soc Am* 1971;61(5):1201–211.
- [95] Richter CF. Site-dependent spectra for earthquake-resistant design. *Bull Seismol Soc Am* 1958;66:221–43.
- [96] Trifunac MD, Lee VW. Frequency dependent attenuation of strong earthquake ground motion. Los Angeles, California: Department of Civil Engineering, University of Southern California; 1985. Rep. no. 85–02.
- [97] Trifunac MD, Lee VW. Direct empirical scaling of response spectral amplitudes from various site and earthquake parameters, US Nuclear Regulatory Commission, Report NUREG/CR-4903, vol. 1, 1987.
- [98] Trifunac MD, Lee VW. Preliminary empirical model for scaling Fourier amplitude spectra of strong ground acceleration in terms of earthquake magnitude, source to station distance, site intensity and recording site conditions. Los Angeles, California: Department of Civil Engineering, University of Southern California; 1985. Rep. no. 85–03.
- [99] Trifunac MD, Lee VW. Preliminary empirical model for scaling pseudo relative velocity spectra of strong earthquake acceleration in terms of magnitude, distance, site intensity and recording site conditions, Rep. no. 85–04, Department of Civil Engineering, University of Southern California, Los Angeles, California, 1985.
- [100] Trifunac MD. Broad band extension of Fourier amplitude spectra of strong motion acceleration Los Angeles, California: Department of Civil Engineering, University of Southern California; . Rep. no. CE 93–01.
- [101] Trifunac MD. Long period Fourier amplitude spectra of strong motion acceleration. *Sol Dyn Earthquake Eng* 1993;12(6):363–82.
- [102] Lee VW, Trifunac MD, Todorovska MI, Novikova EI. Empirical equations describing attenuation of the peaks of strong ground motion, in terms of magnitude, distance, path effects and site conditions Los Angeles, California: Department of Civil Engineering, University of Southern California; . Report CE 95–02.
- [103] Castellaro S, Mulargia F, Rossi PL. Vs30: proxy for seismic amplification? *Seismol Res Lett* 2008;79(4):540–3.